Indian Geotechnical Journal, 35 (3), 2005

Evaluation of Wave Induced Liquefaction Potential of Non-homogeneous Seabeds

Madhab Paul*, Atul Nanda† and Dulal Goldar‡

Introduction

Storm waves can induce substantial cyclic loading on the seabed, which may lead to seabed instability. Seabed consisting of loose sands may liquefy, which may significantly affect the serviceability and stability of marine structures. The probability of seafloor instability due to gravity forces in very weak soils, where the bottom has a moderate slope, was recognized by Terzaghi (1956). Wave induced seafloor instability was recognized in 1969 when Hurricane 'Camille' struck areas around Gulf of Mexico having seabed slope less than 0.5% and offshore structures were damaged due to mud movement. Henkel (1970) was the first to provide an analytical framework for stability analysis under wave loading. The possibility of wave induced liquefaction in ocean floor soils was recognized and analyzed by Bjerrum (1973) in connection with the design of foundations for North Sea structures.

While there are established procedures available for the evaluation of liquefaction potential under seismic loading, this is not the case for wave induced liquefaction. A key difference between wave induced and seismic liquefaction is the large duration of storms as compared to the duration of earthquakes. Therefore, the pore pressure dissipation effects have a significant impact on the results of the wave induced liquefaction analysis. The available procedures for analyzing wave induced liquefaction either do not consider

* Engineers India Ltd., EIB - 2nd Floor, 1 Bhikaji Cama Place, New Delhi – 110066, India. E-mail: madhab.paul@eil.co.in

† Engineers India Ltd., EIB - 2nd Floor, 1 Bhikaji Cama Place, New Delhi – 110066, India. E-mail: ananda@eil.co.in

‡ Department of Civil Engineering, Delhi College of Engineering, New Delhi – 110042, India.

the pore pressure dissipation effects or are too complex to use. The available empirical methods to analyze wave induced liquefaction (Nataraja et al., 1980; Ishihara and Yamazaki, 1984) do not consider pore pressure dissipation effect. Approximate analytical methods (Barends and Calle, 1985; Rahman and Jaber, 1986; Nanda and Paul, 2001) assume linear soil behaviour. Numerical techniques vary from one-dimensional finite difference (Seed and Rahman, 1978), one dimensional FEM (Nanda et al., 2000) to advanced elasto-plastic models (Sassa et al., 2001).

Most of the earlier works in wave induced liquefaction (Barends and Calle, 1985; Rahman and Jaber, 1986; Nanda and Paul, 2001), assume the liquefiable soil layer as a linear homogeneous soil layer. The behaviour of a linear homogeneous sand layer under wave loading is well established and analytical solutions are available for predicting the development pore pressure. The pore pressure ratio in a homogeneous sand layer is a function of a single non-dimensional time parameter (Nanda and Paul, 2001). Also the maximum pore pressure ratio occurs at the surface of the seabed.

However the behaviour of non-homogeneous sand layer is not similar to that of a homogeneous sand layer. Generally, naturally occurring soil deposits are non-homogeneous. Also replacement of part of a potentially liquefiable layer by a free draining non-liquefiable material is often used to mitigate the liquefaction risk. In view of above, a two-layer soil model would be an adequate approximation in many cases. In this paper a nonlinear one-dimensional finite element model has been developed and used to analyze pore pressure development under wave loading on a two layer soil system. The model includes both generation as well as dissipation of pore pressure under wave loading. Influence of permeability, liquefaction resistance of the soil and relative thickness of the two layers on the pore pressure developed are also presented in this paper.

Parametric studies have been carried out. The results of these parametric studies can be used as a reference in evaluating liquefaction potential of naturally occurring deposits as well as for recommending remedial measures against seabed liquefaction due to wave loading.

Finite Element Formulation

The equation governing the generation and dissipation of pore pressure under wave loading is given as (Seed and Rahman, 1978):

$$C_v \frac{\partial^2 u}{\partial z^2} = \frac{\partial u}{\partial t} - q \tag{1}$$

where $C_v = k/g_w m_v$ is the coefficient of consolidation,

k = soil permeability,

m_v = coefficient of compressibility, and

q = rate of generation of pore pressure under undrained conditions:

$$q = \frac{\partial u_g}{\partial t} = \frac{\partial u_g}{\partial N}\frac{\partial N}{\partial t} \tag{2}$$

where u_g = excess pore pressure generated under undrained conditions, and

N = number of cycles.

The term $\partial u_g/\partial t$ can be evaluated using Eqns.3 and 4 as given below:

$$\frac{\partial N}{\partial t} = \frac{N_{eq}}{t_D} = \frac{1}{t_p} \tag{3}$$

where N_{eq} = number of equivalent storm waves,

t_D = total duration of the storm, and

t_p = time period of the waves.

The evolution of pore pressure under undrained condition with the number of cycles can be approximated as (Seed and Rahman, 1978):

$$\frac{u_g}{\sigma_{v_0}} = \frac{2}{\Pi}\arcsin\left\{\left(\frac{N}{N_l}\right)^{1/2\theta}\right\} \tag{4}$$

where N_l = number of cycles required for liquefaction under undrained conditions, and

θ = a constant.

A value of θ = 0.7 has been found to provide a reasonable approximation for many types of sand (Seed and Rahman, 1978).

The term $\partial u_g/\partial N$ is nonlinear and can be evaluated by differentiating Eqn.4. Equation 4 requires an estimate of the number of cycles to liquefy under undrained condition (N_l), which in turn requires evaluation of the cyclic stress ratio induced in the seabed. The cyclic shear stress ratio within the seabed, induced by wave loading can be estimated using elastic theory for a semi-infinite seabed (Seed, 1987; Ishihara and Yamazaki, 1984):

$$\frac{\tau}{\sigma_{v_0}} = \left(\frac{2\pi P_0}{\gamma L}\right) e^{-\left(\frac{2\pi z}{L}\right)} \tag{5}$$

where t = cyclic shear stress,

σ_{v_0} = initial vertical effective stress in the seabed,

γ = unit weight of sand,

Z = depth below the mudline, and

P_0 = wave induced seabed pressure on the seabed.

The wave induced seabed pressure is estimated using linear wave theory for a rigid seabed (Horikawa, 1978):

$$P_0 = \frac{\gamma_w H}{2\cosh\left(\frac{2\pi d}{L}\right)} \tag{6}$$

where H = wave height,

L = wave length,

d = water depth, and

γ_w = unit weight of water.

The undrained cyclic shear strength and the number of cycles to liquefaction, for cyclic stress ratios (τ/σ'_{v_0}), of the seabed sand can be evaluated by conducting cyclic triaxial tests on the sand. Alternatively the relationship between cyclic stress ratio and the number of cycles to liquefaction (N_l) based on Standard Penetration Test (SPT) data may be used, (Nataraja et al., 1980).

The finite element formulation of Eqn.1 leads to:

$$\mathbf{Ku} + \mathbf{C}\frac{\partial \mathbf{u}}{\partial t} = \mathbf{Q} \tag{7}$$

where **K** and **C** are matrices and **Q** is a vector and are given below:

$$\mathbf{K} = C_v \int \frac{\partial N_i}{\partial z} \frac{\partial N_j}{\partial z} dz \tag{8}$$

$$\mathbf{C} = \int N_i N_j dz \tag{9}$$

$$\mathbf{Q} = \int N_l dz \tag{10}$$

where, N_i and N_j are the shape functions.

The above finite element equation can be numerically integrated to evaluate the excess pore pressures u at every time step. It may be noted that the above terms have to be evaluated at every time step, each time step being equal to 0.5 second. The above finite element formulation has been implemented in a program with one-dimensional 2-node linear elements.

This finite element model has been validated by comparing with approximate analytical solution for homogeneous linear soil layer (Nanda and Paul, 2001).

Two Layer Analysis

Analyses considering the sandy seabed consisting of two sand layers, underlain by an impermeable layer, have been carried out. Two-layer analyses have been carried out with various combinations of permeability (k), number of cycles required for liquefaction (N_l) and ratios of thickness (T_{ij}) of top layer to total thickness (B) of the two-layer system, as show in Fig.1.

The liquefaction potential of seabed is evaluated in terms of pore pressure ratio (r_u). The pore pressure ratio at a particular depth in seabed, is the ratio of pore pressure to the effective initial vertical stress, at that depth.

The 10 m thick layer has been represented by 40 number 2-node elements of equal length. Pore pressures were calculated at the nodes and the pore pressure ratio at the middle of each element. Initial pore pressures are zero throughout the layer and the bottom of the base layer is impermeable and the top of the layer is free draining.

Parameters for the Two Layer Analysis

Analyses were carried out using wide range of values of permeability

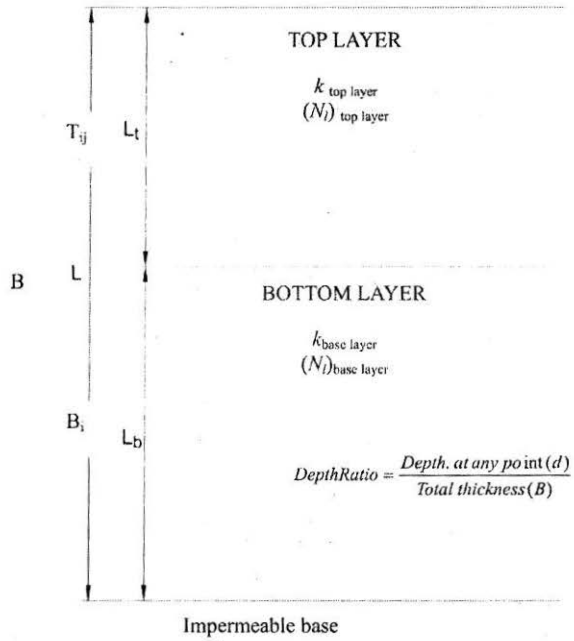

FIGURE 1 : Typical Layer Properties of a Two-Layer System

(k) and number of cycles required for liquefaction (N_l), to cover a range of two layer behaviours. The permeability of the top layer varies from one-tenth to ten times the permeability of the base layer; and N_l of the top layer varies from 10 to 1000. The increasing value of the N_l indicates that the soil is increasingly less liquefiable. Soil having N_l value around 10 is a potentially liquefiable soil; whereas, soil with N_l value around 1000 has high resistance against liquefaction. It may be noted that while k and N_l are not always independent of each other, the above range of parameters have been selected to evaluate the influence of k, N_l and relative layer thickness likely to occur in the field.

Results for the Two Layer Analysis

In the two layer analysis, the combined thickness (B) of the two layers has been considered as 10m. The properties (k and N_l) of the top layer have been varied, keeping the properties of the base layer constant; and analyses were carried out with varying thickness of top and base layer, keeping the total thickness constant.

Two sets of cases have been analyzed. In Case I, the pore pressure ratio (r_u) at the top of the homogeneous 10 m thick base layer is equal to 0.062, which is very small. While, in Case II, the r_u at the top of the homgeneous 10 m thick base layer is equal to 0.536, which is considerable. These two cases have been considered to analyse the influence of low and high values of pore pressures on the response of the two layer system. The two sets of cases along with the soil parameters used in the analyses are tabulated in Table 1. In each set of analyses, the base layer of the two-layer system, having the same permeability k and N_l values has been selected for better comparison of the analytical results. The pore pressure ratios are studied for the two cases – carrying out eight sets of analyses, as per Table 1. For each set of analyses, five analyses are carried out for T_{ij}/B_i equal to 0.0, 0.25, 0.50, 0.75 and 1.0, as shown in Fig.1.

For better comparison of the results, the depth and pore pressure ratio have been normalized as depth ratio and normalized pore pressure ratio, respectively. The depth ratio at any point is the depth of that point divided by the total thickness of the two layers, i.e., 10 m (Fig.1). The pore pressure ratios in a two-layer system are normalized with respect to the pore pressure ratio, at top, of the base layer having thickness equal to the thickness of the two-layer system , i.e., 10 m. Also let r_{ub} be the pore pressure ratio for the homogenous case, when the whole layer consists of material of base layer and r_{ut} be the pore pressure ratio for the homogenous case, when the whole layer consists of material of the top layer.

The results of the above analyses are presented below. All analyses are carried out till either the pore pressure reaches a steady state or till the initiation of liquefaction within the soil layer, as both the situations are of practical interest.

TABLE 1 : Properties of Two Layer System

Case No	Base Layer			Top Layer		
	Layer	k (m/s)	N_l	Layer	k (m/s)	N_l
I(a)	B_1	3×10^{-3}	10	T_{11}	3×10^{-4}	10
I(b)	B_1	3×10^{-3}	10	T_{12}	3×10^{-2}	10
I(c)	B_1	3×10^{-3}	10	T_{13}	3×10^{-4}	1000
I(d)	B_1	3×10^{-3}	10	T_{14}	3×10^{-2}	1000
II(a)	B_2	2×10^{-4}	10	T_{21}	2×10^{-5}	10
II(b)	B_2	2×10^{-4}	10	T_{22}	2×10^{-3}	10
II(c)	B_2	2×10^{-4}	10	T_{23}	2×10^{-5}	1000
II(d)	B_2	2×10^{-4}	10	T_{24}	2×10^{-3}	1000

Results for the Case I

In this case, the pore pressure ratio in the 10 m thick base layer, is very small and the r_{ub} value varies from 0.062 (at top) to 0.043 (at bottom). Figures 2, 3, 4 and 5 present the normalized pore pressure ratio versus depth ratio plots for the four sets of analyses. Figure 2 presents the results of Case I(a), when the top layer has the same liquefaction resistance (N_l) as that of the base layer, but ten times lower permeability than that of the base layer. Due to generation of pore pressure, pore water moves upward into the top layer at a rate faster than the rate at which it can dissipates through the top layer. With the increase in thickness of top layer the behavior of the two-layer approximates towards the behavior of a single layer consisting of top layer material. Hence for Case I(a), the value of r_u in two layer increases throughout the layer as compared to the value of r_{ub}; and tends towards corresponding value of r_{ut}. In the top layer, r_u in the case of top layer to base layer thickness ratio of 0.25 and 0.50, is slightly more than r_{ut}. The value of r_u at the top of the two-layer is 6.49, 5.87 and 5.69 times the r_{ub} value at top for top layer to base layer thickness ratio 0.25, 0.50, and 0.75 respectively.

In Case I(b), the top layer has the same liquefaction resistance (N_l) as that of the base layer but ten times higher permeability than that of the base layer. Due to generation of pore pressure, pore water moves upward into the

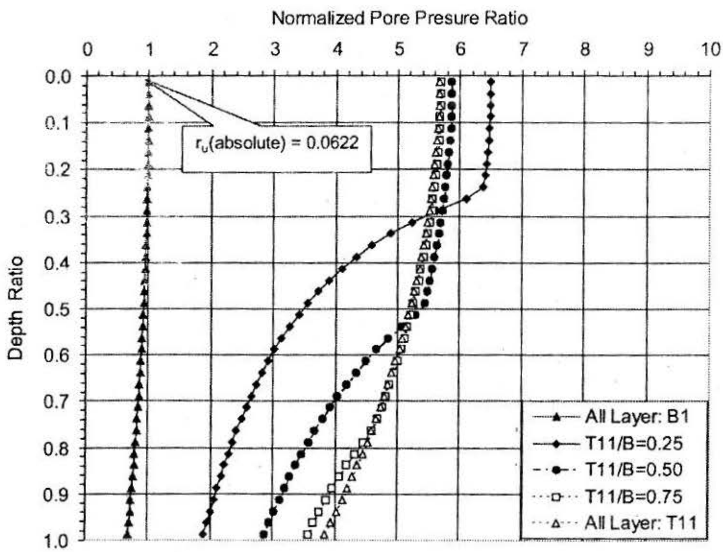

FIGURE 2 : Depth Ratio vs. Normalized Pore Pressure Ratio Plots for Top Layer T_{11} (k = 3 × 10^{-4} m/s; N_l = 10) and Base Layer B_1 (k = 3 × 10^{-3} m/s; N_l = 10), Case I(a)

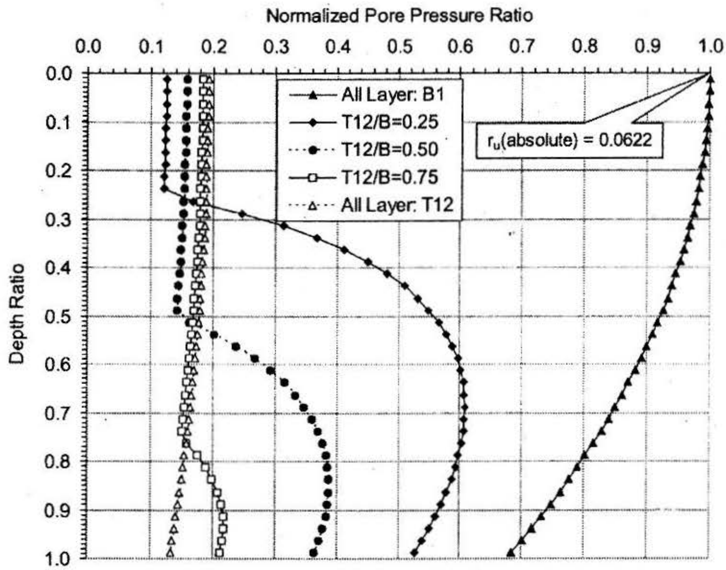

FIGURE 3 : Depth Ratio vs. Normalized Pore Pressure Ratio Plot for Top Layer T_{12} ($k = 3 \times 10^{-2}$ m/s; $N_l = 10$) and Base Layer B_1 ($k = 3 \times 10^{-3}$ m/s; $N_l = 10$), Case I(b)

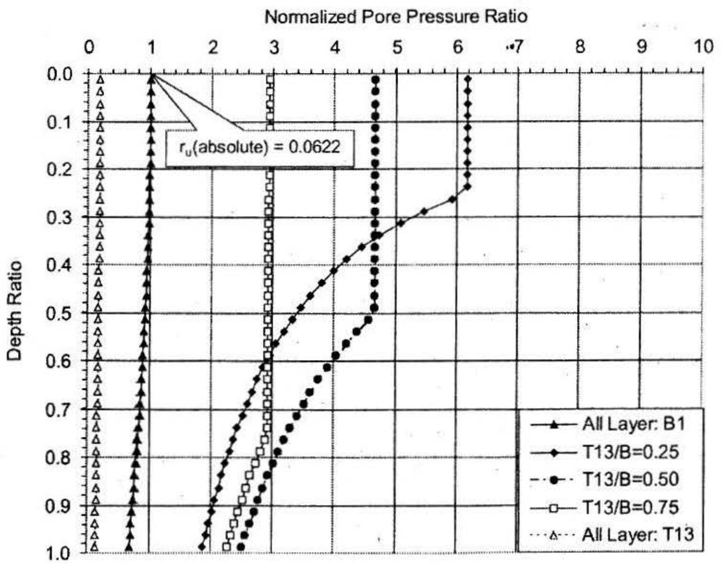

FIGURE 4 : Depth Ratio vs. Normalized Pore Pressure Ratio Plot for Top Layer T_{13} ($k = 3 \times 10^{-4}$ m/s; $N_l = 1000$) and Base Layer B_1 ($k = 3 \times 10^{-3}$ m/s; $N_l = 10$), Case I(c)

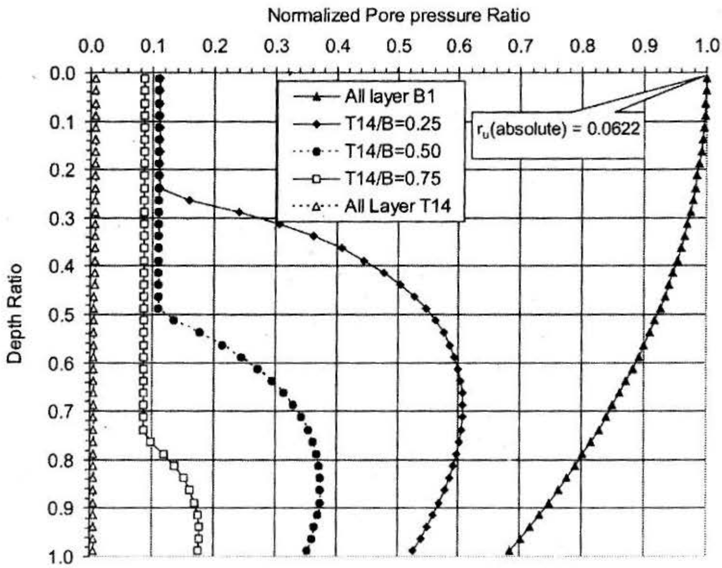

FIGURE 5 : Depth Ratio vs. Normalized Pore Pressure Ratio Plot for Top Layer T_{14} ($k = 3 \times 10^{-2}$ m/s; $N_l = 1000$) and Base Layer B_1 ($k = 3 \times 10^{-3}$ m/s; $N_l = 10$), Case I(d)

top layer and dissipates through the top layer at a rate faster than in the base layer. As a result it can be observed that (Fig.3):

(i) magnitude of the pore pressure ratio (r_u), in the two layer system, decreases,

(ii) the value of r_u in the base layer is less than the corresponding r_{ub}; while it is more than the corresponding value of r_{ut},

(iii) the value of r_u in the top layer is slightly less than the corresponding value of r_{ut}, and

(iv) with increasing thickness of the top layer, the value of r_u in the two layer system, gets closer to the corresponding value of r_{ut}, as the two-layer system approximates towards a single layer consisting of top layer material only.

However, when the top layer has lower permeability and higher liquefaction resistance than that of the base layer, as in Case I(c), the pore pressure ratio in the two layer system becomes much higher than the corresponding values of both r_{ut} and r_{ub} as shown in Fig.4. At the top, the value of r_u in the two layer system, becomes 6.19, 4.66, 2.94 times the corresponding value of r_{ub} , for the ratio of top layer to base layer thickness of 0.25, 0.50, and 0.75 respectively. In this case, the value of r_{ut} at the top of the layer is only 0.193 times that of the corresponding value of r_{ub} due to the high N_l value. This is a very interesting and important case. In this case, the combination of two-layer is more susceptible to liquefaction. The pore pressure increases through out the layer as the pore water can not dissipate through the top layer as fast as it can dissipate through the bottom layer. The top layer material has very high resistance to liquefaction (N_l value equal to 1000) and hence there is insignificant development of pore pressure in this layer. Therefore, when the whole layer is replaced by a top layer material, there is practically no development of pore pressure throughout the layer.

In Case I(d), when the top layer has higher permeability and higher liquefaction resistance than that of the base layer, it can be observed from Fig.5 that the pore pressure ratio in the two layer system is much higher than the corresponding values of r_{ut} but lower than the corresponding values of r_{ub}. The r_{ut} values become negligible as the N_l value is equal to 1000. At top of the two layer system, the value of r_u becomes 0.11, 0.11, 0.087 times the corresponding value of r_{ub}, for the ratio of top layer to base layer thickness of 0.25, 0.50, and 0.75, respectively.

In all the above four cases, in the two layer system, the pore pressure ratio in the top layer remains almost constant with the depth of top layer, while it varies nonlinearly in base layer with depth.

Results for the Case II

In this case, the pore pressure ratio in the 10 m thick base layer, is considerable; and the r_{ub} value varies from 0.536 (at top) to 0.357 (at bottom). Figures 6, 7, 8 and 9 present the normalized pore pressure ratio versus depth ratio plots for the four sets of analysis. As the r_u value is high in Case II, complete liquefaction occurs in many cases.

The results of Case II(a), when top layer has the same liquefaction resistance (N_l) as that of the base layer, but ten times lower permeability than that of the base layer, are presented in Fig.6. In this case, soil liquefies at the interface of the two-layer, and simultaneously liquefaction extends slightly into the top layer, when the ratio of thickness of the top layer to total thickness of the two-layer are 0.25 and 0.50. The value of r_u decreases above and below the liquefaction zone. Soil starts to liquefy near the middle of two-layer, and simultaneously liquefaction extends upto top of the layer, when the ratio of thickness of the top layer to total thickness of the two-layer is 0.75; a similar trend is also observed when the complete layer is replaced by the top layer material.

In Case II(b), the top layer has the same liquefaction resistance (N_l) as of base layer but ten times higher permeability than that of the base layer, and the results (Fig.7) show a similar trend as observed in Case I(b), (Fig.3). Liquefaction does not occur in these cases.

However, when the top layer has lower permeability and higher liquefaction resistance (N_l) than that of the base layer, Case II(c), the r_{ut} value at the top is 0.156 times that of r_{ub} value at the top. Individually both top and bottom layer may not liquefy, however their combination becomes more susceptible to liquefaction. In this case, as observed in Case I(c), through the top layer the pore water can not dissipate as fast as it can dissipate through bottom layer. Consequently pore pressure accumulates near the interface and maximum pore pressure is also observed at the interface. In this case, the pore pressure ratio at the interface of the two-layer, becomes equal to one, i.e., soil liquefies (Fig.8). Both above and below the interface of the two-layer, the pore pressure ratio again decreases. At the top, the value of r_u in the two layer system, becomes 1.52, 0.98, and 0.72 times the corresponding value of r_{ub}, for the ratio of top layer to base layer thickness of 0.25, 0.50, and 0.75 respectively. While at bottom, the value of r_u in the two layer system, becomes 0.63, 1.05, and 1.44 times the corresponding value of r_{ub}, for the ratio of top layer to base layer thickness 0.25, 0.50, and 0.75 respectively. This pattern needs to be kept in mind while designing remedial measures against liquefaction of seabed.

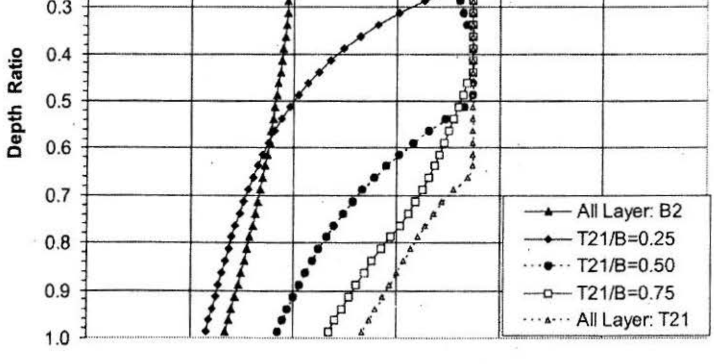

FIGURE 6 : Depth Ratio vs. Normalized Pore Pressure Ratio Plots for Top Layer T_{21} (k = 2 × 10^{-5} m/s; N_l = 10) and Base Layer B_2 (k = 2 × 10^{-4} m/s; N_l = 10), Case II(a)

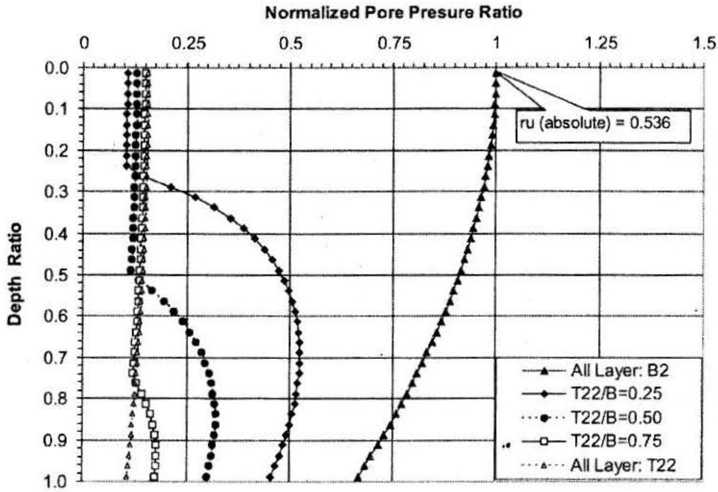

FIGURE 7 : Depth Ratio vs. Normalized Pore Pressure Ratio Plot for Top Layer T_{22} ($k = 2 \times 10^{-3}$ m/s; $N_l = 10$) and Base Layer B_2 ($k = 2 \times 10^{-4}$ m/s; $N_l = 10$), Case II(b)

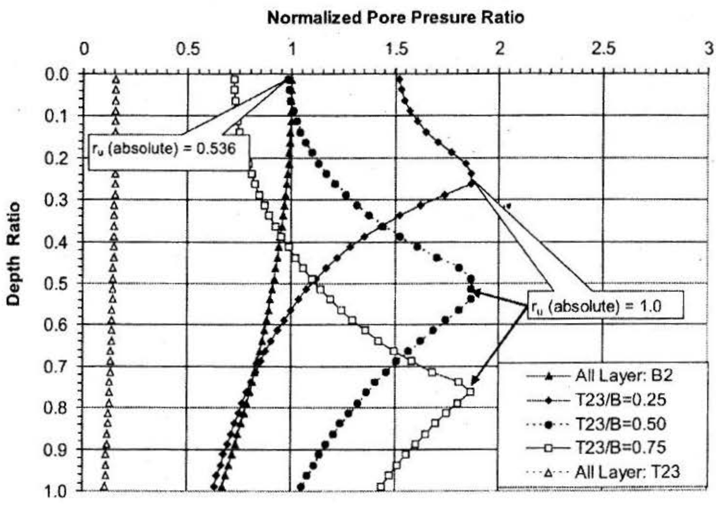

FIGURE 8 : Depth Ratio vs. Normalized Pore Pressure Ratio Plot for Top Layer T_{23} ($k = 2 \times 10^{-5}$ m/s; $N_l = 1000$) and Base Layer B_2 ($k = 2 \times 10^{-4}$ m/s; $N_l = 10$), Case II(c)

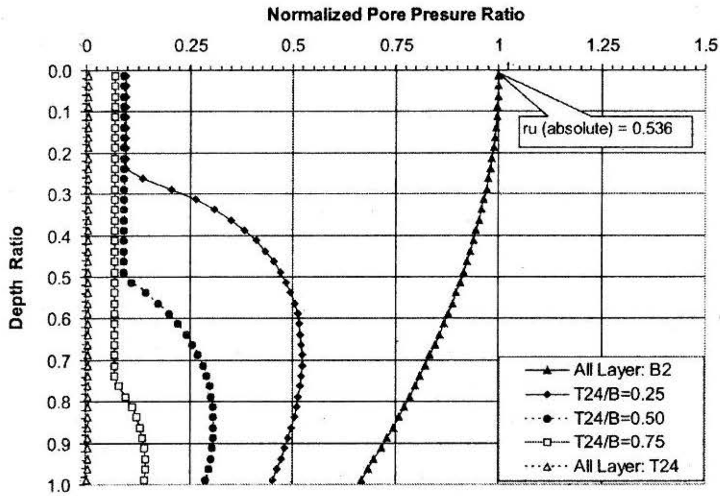

FIGURE 9 : Depth Ratio vs. Normalized Pore Pressure Ratio Plot for Top Layer T_{24} (k = 2 × 10^{-3} m/s; N_l = 1000) and Base Layer B_2 (k = 2 × 10^{-4} m/s; N_l = 10), Case II(d)

In Case II(d), when the top layer has higher permeability and higher liquefaction resistance (N_l) than that of base layer, it can be observed from Fig.9, that the pore pressure ratio in the two layer system becomes much more than the corresponding values of r_{ut} and but less than the corresponding value of r_{ub} as observed earlier in Case I(d), (Fig.5). At the top of the two layer system, the value of r_u becomes 0.096, 0.091, and 0.071 times the corresponding value of $r_{ub,}$ for the ratio of top layer to base layer thickness 0.25, 0.50, and 0.75, respectively. In this case, r_{ut} at top is 0.006 times that of r_{ub} at top of the layer.

In Cases II(b) and II(d), liquefaction does not occur; and the pore pressure ratio in the top layer remains constant, while it varies nonlinearly with depth in base layer, as observed in all four set of analyses of Case I.

Generation of Pore Pressure with Time

Pore pressure development with time has been studied. In the pore pressure ratio versus time plots, the time step is maintained as 0.5 second. It has been observed that the pore pressure is gradually built up in the seabed and any of the following two situations may occur:

a) Pore pressure ratio reaches a steady state with a peak value below one, i.e., soil does not liquefy, as observed in all the analyses of Cases I(a), I(b), I(c) and I(d), as well as of Cases II(b) and II(d). In all these cases

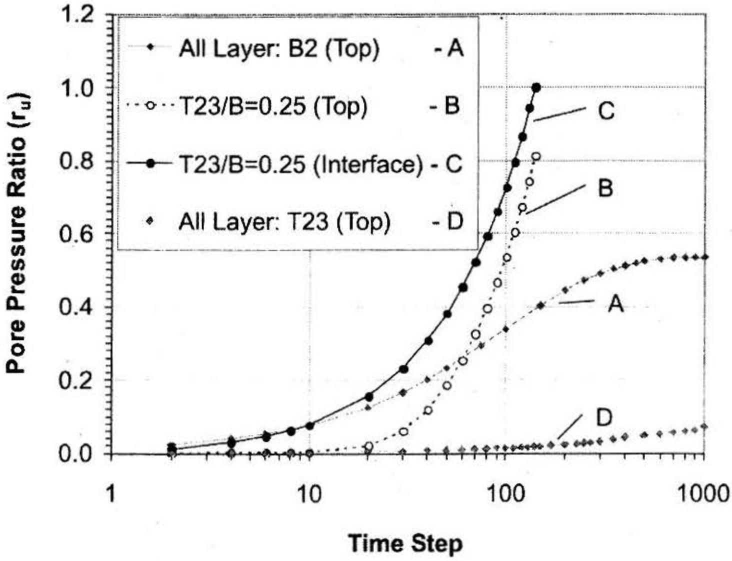

FIGURE 10 : Pore pressure Ratio vs. Time Plots for Top Layer T_{23} ($k = 2 \times 10^{-5}$ m/s; $N_l = 1000$) and Base Layer B_2 ($k = 2 \times 10^{-4}$ m/s; $N_l = 10$) combination, Case II(c)

the pattern of the pore pressure ratio versus time plots is similar to that of curve (A) and (D) as shown in Fig.10.

b) Pore pressure ratio becomes equal to one, i.e., soil liquefies at some level in the two-layer, as observed in two cases, Cases II(a) and II(c). In these cases, the pore pressure ratio rapidly increases with time and approaches unity, i.e., liquefaction.

Conclusion

Parametric studies have been carried out to evaluate liquefaction potential of a non-homogeneous seabed. The non-homogenous seabed has been idealized as a two-layer system. The results of two-layer analyses illustrate the complex behavior of non-homogeneous seabed subjected to wave loading. The pore pressure developed in the seabed depends not only on the permeability (k) and cyclic strength of the material (N_l) of the seabed, but also on the relative thickness of the two layers. Also the location of the maximum pore pressure ratio is not always at surface of the seabed as normally observed in case of homogeneous soil, but in some cases maximum pore pressure develops at the interface of the two layers. This can clearly be observed when the top layer has lower permeability than the bottom layer and the pore pressure ratio in the bottom layer is high.

When the top soil is replaced by a soil of lower permeability but having the same liquefaction resistance as that of the base layer, the pore pressure ratio increases through out the two-layer. The increase in pore pressure ratio is also significant when part of the layer is replaced by a top soil layer which has lower permeability as well as higher liquefaction resistance than that of the base layer. However, when the top portion of the base layer is replaced with a more permeable layer, the pore pressure ratio in the soil reduces, and in this case, the liquefaction resistance of the top soil does not have significant impact on the results.

The above analysis can also be used in the design of remedial measures against wave induced liquefaction, such as partial replacement of potentially liquefiable layers by non-liquefiable materials and also for naturally occurring soil deposits.

The results presented in this paper indicate the general pattern. The graphs presented can not be directly used to evaluate the liquefaction potential of a particular site. Detailed analysis needs to be carried out to evaluate the liquefaction potential of a particular site.

Acknowledgement

The authors would like to thank the management of Engineers India Limited for granting permission to carry out this research work and to publish this paper.

References

BARENDS, F.B.W. and CALLE, E.O.F. (1985) : "A Method to Calculate the Geotechnical Stability of Offshore Structures founded on Loosely Packed Seabed Sand in a Wave Loading Environment", *Proc. 4th. Int. Conference on Behaviour of Offshore Structures,* Delft, Netherlands.

BJERRUM, J. (1973) : "Geotechnical Problem involved in Foundation of Structures in the North Sea", *Geotechnique,* Vol.23(3), pp.319-358.

HENKEL, D.J. (1970) : "The Role of Waves in causing Submarine Land Slides", *Geotechnique*, Vol. 20(1), pp.75-80.

HORIKAWA, K. (1978) : *Coastal Engineering,* University of Tokyo Press.

ISHIHARA, K. and YAMAZAKI, A. (1984) : "Analysis of Wave Induced Liquefaction in Seabed Deposit of Sand", *Soils and Foundations*, Vol.24(3), pp.85-100.

NANDA, A. and PAUL, M. (2001) : "Evaluation of Wave Induced Liquefaction Potential", *15^{th} International Conference on Soil Mechanics and Geotechnical Engineering*, Turkey, pp.2243-46.

NANDA, A., PAUL, M. and BHOWAL, S. (2000) : "Wave Induced Seabed

Instability", *Proc. of the Tenth Int. Offshore and Polar Engineering Conference*, Seattle, USA, Vol.2, pp.590-593.

NATARAJA, M.S., SINGH, H. and MATONEY, D. (1980) : "Ocean Wave Induced Liquefaction Analysis: A Simplified Procedure", *Int. Symp. Soils under Cyclic and Transient Loading*, Swansea, Vol.2, pp.509-16.

RAHMAN, M.S. and JABER, W.Y. (1986) : "A Simplified Drained Analysis for Wave Induced Liquefaction", *Soils and Foundations*, Vol.26(3), pp.57-68.

SASSA, S., SEKIGUCHI, H. and MIYAMOTA, J. (2001) : "Analysis of Progressive Liquefaction as a Moving-Boundary Problems", *Geotechnique*, Vol.51(10), pp.847-857.

SEED, H.B. (1987) : "Design Problems in Soil Liquefaction", *J. Geotech. Engg. Div.*, ASCE, Vol.113(8), pp.827-45.

SEED, H.B. and RAHMAN, M.S. (1978) : "Wave Induced Pore Pressures in relation to Ocean Floor Stability of Cohesion Less Soils", *Marine Geotech.*, Vol.3(2), pp.123-50.

TERZAGHI, K. (1956) : "Varieties of Submarine Slope Failure", *Publ. No. 25, Osolo: NGI*, pp.1-16.

Notations

C_v	=	coefficient of consolidation
k	=	soil permeability
m_v	=	coefficient of compressibility
q	=	the rate of generation of pore pressure under undrained conditions
u_g	=	excess pore pressure generated under undrained conditions
N	=	the number of cycles of waves
N_{eq}	=	the number of equivalent storm waves
t_D	=	total duration of the storm
t_p	=	time period of the waves
N_l	=	number of cycles required for liquefaction under undrained conditions
θ	=	a constant.
τ	=	cyclic shear stress
σ_{v_0}	=	initial vertical effective stress in the seabed
τ/σ'_{v_0}	=	cyclic stress ratios

γ	=	unit weight of sand
Z	=	depth below the mudline
P_0	=	wave induced seabed pressure on the seabed
H	=	wave height
L	=	wave length
D	=	water depth
γ_w	=	unit weight of water
T_{ij}	=	thickness of top layer of the two-layer-system
B_i	=	thickness of base layer of the two-layer-system
B	=	total thickness of the two-layer-system
r_u	=	pore pressure ratio
r_{ub}	=	pore pressure ratio when the whole layer consists of material of base layer
r_{ut}	=	pore pressure ratio when the whole layer consists of material of the top layer.
K	=	matrix
C	=	matrix
Q	=	vector